RSC Advances

ROYAL SOCIETY OF CHEMISTRY

www.rsc.org/advances

Graphic Abstract

A novel supramolecular hydrogel AD-g-HPG/CD-g-Dex based on host-guest interaction as scaffold for cell proliferation and drug delivery.

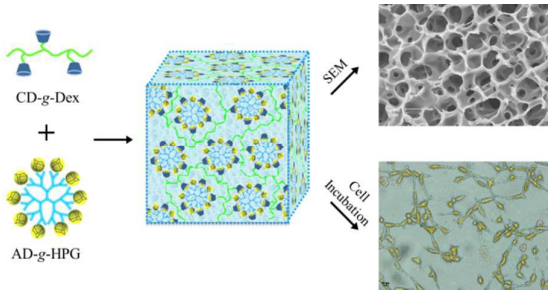

The supramolecular hydrogel based on hyperbranched polyglycerol and dextran as a scaffold for living cells and drug delivery

Jing Li,[a] Huimin Li,[a] Xiaoyuan Yang,[a] Pingyan Luo,[a] Zhongming Wu [a,*] Xinge Zhang,[b]

[a] 2011 Collaborative Innovation Center of Tianjin for Medical Epigenetics (Ministry of Health), Key Laboratory of Hormones and Development, Metabolic Diseases Hospital & Tianjin Institute of Endocrinology, Tianjin Medical University, Tianjin 300070, China.

[b] Key Laboratory of Functional Polymer Materials of Ministry Education, Institute of Polymer Chemistry, Nankai University, Tianjin 300071, China

[*]Corresponding author

Key Laboratory of Hormones and Development Ministry of Health, Metabolic Diseases Hospital, Tianjin Medical University, Tianjin 300070, China

Tel.: +86 22 23343729; Fax: +86 22 23343729.

E-mail: wuzhongming@tmu.edu.cn

Abstract

Hydrogels are good candidates to satisfy many needs for functional and tunable biomaterials. How to precisely control the gel structure and functions is crucial for the construction of sophisticated soft biomaterials comprising supramolecular hydrogels, which not only facilitate the impact of the surrounding environment on a unique biological function occurring, but also manipulate various biological phenomena. Here, we designed and synthesized a new supramolecular hydrogel (AD-*g*-HPG/CD-*g*-Dex) based on hyperbranched polyglycerol and dextran using the association of *β*-cyclodextran with adamantine. AD-*g*-HPG/CD-*g*-Dex hydrogel with the typical porous structure and ideal three-dimensional network showed a rapid increase in equilibrium of swelling, which was up to 185% after 2 min incubation. The hydrogel could encapsulate the protein drug and controlled drug release by modifying the compositions. Importantly, the viability of NIH 3T3 cells was more than 80% after treatment with AD-*g*-HPG/CD-*g*-Dex hydrogel, displaying good cytocompatibility. Taken together, we confirmed the feasibility of cytocompatible AD-*g*-HPG/CD-*g*-Dex hydrogel as a platform scaffold with controlled drug delivery and other various tissue engineering applications.

Keywords: supramolecular hydrogel; host-guest interaction; cell proliferation; drug delivery

Introduction

The continual advances in tissue engineering and regenerative medicine are driving an increasing demand for functional and tunable biomaterials. Hydrophilic hydrogels have been of special interest due to their unique properties and potential applications. In particular, the supramolecular hydrogels based on the self-assembly of the inclusion complexes between cyclodextrins (CDs) with various polymers have parked growing interest in recent years. For example, Li et al. developed a CD-based supramolecular hydrogel system with active cationic copolymer/plasmid DNA polyplexes as a sustained gene delivery carrier.[1] Wu et al. used CD and methoxypolyethylene-glycol-poly(caprolactone)-(dodecanedioicacid)-poly(caprolacto ne) methoxypoly(ethylene glycol) triblock polymers to fabricate the supramolecular hydrogels for stem cell encapsulation.[2] Ma et al. used poly(ethylene glycol) methyl ether/heparin conjugate and CD to obtain supramolecular hydrogels for drug delivery.[3] The self-healing supramolecular hydrogels made of copolymers of *N,N*′-dimethylacrylamide modified with cholic acid and *β*-CD were conducted by Jia et al.[4] Zhang et al. reported the assembly of a thermoresponsive reversible supramolecular architecture through inclusion complexation between star-shaped adamantyl-terminated 8-arm poly(ethylene glycol) (PEG) and star-shaped poly(*N*-isopropylacrylamide) with β-CD core.[5] To date, many supramolecular hydrogels are limited in applications on account of complicated synthesis, the choice of guests and potential toxic metal ions used for their construction.[6] In contrast, much less attention has been paid to the design and preparation of the supramolecular

hydrogels mimicking the extracellular matrix (ECM) used for the tissue engineering.

The polyether backbone of hyperbranched polyglycerol (HPG), taking the biocompatibility of polyether structures such as PEG into account, makes it an attractive polymer for biomedical and pharmaceutic applications. However, HPG shows similar protein-resistant and thrombocyte-activating performance with PEG due to the constitution of a flexible aliphatic polyether backbone with hydrophilic surface groups.[7] Therefore, although this spherical molecule bears hydroxyl groups on the periphery and highly branched architecture allowing modification for end user purposes like many other hyperbranched polymers,[8-9] HPG has been widely used as highly protein-resistant materials to coat on gold,[10] glass,[11] and poly(etherimide)[12] surfaces in the past but seldom been applied in tissue engineering and cell proliferation, especially in the form of supramolecular hydrogel.

In the present work, to prepare a supramolecular hydrogel mimicking ECM and expand the application of HPG in tissue engineering, we designed and synthesized a novel supramolecular hydrogel based on hyperbranched polyglycerol (HPG) and dextran (Dex) using the association of β-cyclodextran (β-CD) with adamantine (AD) in the present work. Importantly, the polysaccharide Dex is chemically similar to glycosaminoglycan which is an important constituent of ECM and have been widely applied in drug controlled release, tissue engineering and scaffolds.[13] It should be noted that the fabrication of supramolecular hydrogel was easily available for the mild preparation conditions and easy-controlled gelation process by host-guest interaction. The cell survival and proliferation in the hydrogel were analyzed using MTT method.

Finally, the feasibility of AD-*g*-HPG/CD-*g*-Dex hydrogel as a platform scaffold with controlled drug delivery and tissue engineering applications was evaluated.

Materials and Methods

Materials

Glycidol, 1,1,1-trimethylolpropane, 4-dimethylaminopyridine (DMAP), Dex, 1-adamantanecarbonyl-chloride, *β*-CD, acridine orange (AO) and ethidium bromide (EB) were purchased from Shanghai Aladdin Industrial Co., China. 3-(4,5-Dimethylthiazol-2-yl)-2,5-diphenyltetrazolium bromide (MTT) was purchased from Sigma-Aldrich, USA. Dulbecco's modified eagle's medium (DMEM), heat-inactivated fetal bovine serum (FBS), penicillin-streptomycin liquid, non-essential amino acid and trypsin were purchased from Gibco, USA. *β*-CD and dimethyl sulfoxide (DMSO) were purchased from Tianjin Rionlon Chemical Ltd., China. Amberlite IRC-50 exchange resin was obtained from Jiangsu Success Resin Ltd., China. Methanol, 1,4-dioxane, acetone, pyridine, KIO_3, tetrahydrofuran and ethylenediamine (EDA) were all purchased from Tianjin Fine Chemical Co., Ltd., China. All the reagents were used of analytical grade.

Preparation of AD-*g*-HPG

Hyperbranched polyglycerol with a molecular weight of 70 kDa (HPGs, Mw/Mn = 2.0) was prepared using the anionic ring-opening polymerization of glycidol in the presence of alkosides according to a previously reported method.[14] Briefly, 1,1,1-tris(hydroxymethyl)propane (0.1023 g) was partially deprotonated (10%) with potassium methylate solution by distilling off excess methanol. 5 mL of glycidol was

added at 95 °C slowly over 12 h. The resulting product was dissolved in methanol and neutralized by filtration over Amberlite IRC-50 exchange resin. The resultant polymer was twice precipitated with acetone, and subsequently dried.

500 mg of HPG was dissolved in 8 mL of pyridine followed by adding 190 mg of DMAP at 0 °C under nitrogen atmosphere. Then, 2 mL of 1-adamantanecarbonyl-chloride (AD, 136 mg) was dropwise added into the above solution, and reacted at room temperature for 24 h. The product was dialyzed against distilled water for 3 days, then precipitated with acetone three times and dried in vacuum. AD-*g*-HPGs were obtained by modifying molar ratio of HPG to AD.

Preparation of CD-*g*-Dex

Mono-6-deoxy-6-ethylenediamino-*β*-CD was prepared by a literature procedure.[15] 120 mg of mono-6-deoxy-6-ethylenediamino-*β*-CD was reacted with Dex oxidized by KIO_3 for 24 h at room temperature. The product was obtained after the reaction mixture was dialyzed for 3 days and freeze dried.[16] *β*-CD content in polymer was 10.3% measured by UV-2550 spectrophotometer (Shimadzu, Japan) according to the reported method.[17]

Synthesis and characteristic of AD-*g*-HPG/CD-*g*-Dex hydrogel

To evaluated the gelation, the solution of AD-*g*-HPG (10%, 15% and 20%), and CD-*g*-Dex (20%) were incubated in phosphate buffer solution (PBS, pH 7.4, 0.02 M) at 37 °C by oscillation. The gelation time was determined by a flow text utilizing a glass test tube inverting method reported by Jeong et al.[18] The sample was regarded as a gel when the solution lost fluidity in 1 min.

^{1}H-NMR spectra of the monomers and copolymers in D_2O were obtained with a Varian Unity Plus-400 MHz spectrometer. FTIR spectroscopy of the sample was performed with FTS 6000 spectrometer (Bio-Rad, USA). The dried samples were mixed with KBr and tabled. To examine thermal stability of hydrogels, the samples were measured using thermogravimetric analysis (TGA, Metzsh). Decomposition profiles of TGA were recorded with a heating rate of 10 °C /min in nitrogen between 20 and 1000 °C. UV absorption spectrum was measured using a UV spectrophotometer (UV-2550) from Shimadzu.

Rheological measurements

Rheology measurements were carried out by an Advanced Rheometer (TA Instruments Inc. AR2000ex, USA) with a 40 mm steel plate. To be a basic characterization for hydrogel, the dynamic rheology property of all kinds of AD-*g*-HPG/CD-*g*-Dex supramolecular hydrogel was investigated in terms of the storage modulus (G') and loss modulus (G'') with an angular frequency from 0.1 to 100 rad/s. All measurements were performed at temperature at 25 °C.

Morphology observation

To observe the morphology of hydrogels, the synthetic hydrogels were quickly frozen in liquid nitrogen and further dried in a Freeze Drier (FTS SYSTEMS, USA) in vacuum at -90 °C for overnight until all the solvent was sublimed. The morphology of the dried hydrogels was visualized by using a scanning electron microscope (SEM, Shimadzu SS-550, Japan).[19] Before observed with the SEM, the hydrogel samples were fixed on conductive tape and coated with gold.

Swelling ratio of hydrogel

To understand the effect of the molecular transport of liquids into hydrogels on the cell culture and drug release, swelling measurement was performed by immersing the hydrogels in pH 7.4 PBS at 37 °C. At predetermined time intervals, the samples were taken out and wiped carefully between tissue papers to remove the surface-adhered liquid droplets, and then weighted on an electron microbalance (AE 240, Mettler, Switzerland) to an accuracy of ± 0.1 mg. Each sample was performed in triplicate, and average value was calculated for data analysis. The percentage of equilibrium water uptake was calculated as follows:

$$\text{Swelling ratio (\%)} = \frac{W_t - W_0}{W_0} \times 100\ \%$$

where W_t is the weight of swollen hydrogels, and W_0 is the initial weight of hydrogels.[20]

In vitro degradation

The degradation of AD-*g*-HPG/CD-*g*-Dex hydrogel in buffer solution was determined by mass loss. Hydrogel samples were prepared at a 2 mm thickness and 1 cm diameter and weighted, and then incubated in 2 mL PBS (pH 7.4). The samples were maintained at 37 °C and 100 rpm and the buffer was replenished weekly. After the 1, 3, 5, 7, 10 and 14 days of incubation, the samples were removed, patted dry and weighed. Each sample was performed in triplicate, and average value was calculated for data analysis. Degradation percentage was determined using following equation:

$$\text{Degradation (\%)} = \frac{W_0 - W_t}{W_0} \times 100\ \%$$

where W_t is the dry weight of hydrogels at different predetermined time, and W_0 is the initial weight of hydrogels.

Insulin encapsulation and in vitro release

To explore AD-*g*-HPG/CD-*g*-Dex hydrogel as a vehicle for drug delivery, insulin, as a model drug, was encapsulated into hydrogels. Briefly, 9 mg insulin was added to 10 mL of PBS (pH 7.4), then AD-*g*-HPG and CD-*g*-Dex were dissolved in the solution and the mixture was incubated at 37 °C by oscillation to obtain drug-loaded hydrogels. In this case, the drug loading capability was considered to be 100%.

To investigate the insulin release from the hydrogel, 6 mg of insulin-encapsulated hydrogel was immersed in 2 mL of PBS (pH 7.4) under 100 rpm shaking at 37 °C. At predetermined time, 100 μL of supernatant was withdrawn and replaced with the same volume of fresh medium. The amount of free insulin was determined by the Bradford method[21] and a calibration curve was generated using blank hydrogel to correct for the intrinsic absorption of the polymer. Each sample was analyzed in triplicate.

Circular dichroism spectroscopy

To confirm whether encapsulated insulin in AD-*g*-HPG/CD-*g*-Dex hydrogel could maintain its conformation and activity, native insulin and released insulin were estimated by J-810 circular dichroism spectrophotometer (Jasco, Japan) at 25 °C with a cell length of 0.1 cm. The standard insulin solution was prepared in pH 7.4 PBS to a final concentration of 0.1 mg/mL. For the far-UV circular dichroism spectra, samples were scanned from 190 to 260 nm and accumulated 10 times, at a resolution of 1.0 nm

and scanning speed of 100 nm/min. All circular dichroism data are expressed as mean residue ellipticity.[22]

Cytotoxicity

Mouse fibroblast NIH 3T3 cells were cultivated in DMEM supplemented with 10% FBS, 100 mg/L streptomycin, and 100 IU/mL penicillin under moist atmosphere (5% CO_2/95% air). The cell suspension (5×10^4 cells per mL) was seeded into 96-multiwell culture plate and cultured in an incubator for up to 24 h. Before cell seeding, 8 mg of hydrogels were incubated in 8 mL of pH 7.4 PBS for 72 h, and then filtrated to get hydrogel leaching solution. Cell viability was evaluated by MTT biochemical assay. At 24 h after seeding, the culture medium was replaced with the different concentrations of hydrogel leaching solution (0.625, 1.25, 2.5 and 5.0 mg/mL), the control group only added an equal amount DMEM medium cultured in 5% CO_2/95% air incubator for 48 h. Then, 10 μL of MTT solution (5%) in PBS was added to the above mixture, and the cells were further incubated for another 4 h. Afterwards, the MTT solution was replaced with 200 μL of DMSO and the 96-multiwell plate was shaken until complete salt crystal dissolution was obtained. Absorbance was measured using Microplate Reader (Molecular Devices, USA; test wavelength: 545 nm; reference wavelength: 630 nm). The number of surviving cells was expressed as percent viability = $(A_t-A_0)/(A_c-A_0)\times100\%$. Where A_t is the absorbance of treated cell, A_c is the absorbance of controlled cell and A_0 is the absorbance of PBS.

Cell viability assay

LIVE/DEAD assay was used to evaluate the cytocompatibility of hydrogel. NIH 3T3

cells were dissociated from culture flasks by trypsin, then counted and suspended in medium at a concentration of 5×10^4 cells per mL. AD-*g*-HPG and CD-*g*-Dex were sterilized by ultraviolet radiation for 2 h, and then dissolved in 200 μL of the cell suspension. 500 μL of medium was added to the cell-encapsulated hydrogel, and subsequently co-cultured for 48 h. 400 μL of AO/EB mixed solution (0.1 mg of AO and 0.1 mg of EB dissolved in 100 μL of pH 7.4 PBS) was added after removing the cell culture medium. After 5 min, hydrogel was washed with pH 7.4 PBS three times. The live/dead cells were determined using DMI4000B fluorescence microscope (Leica, Germany).[23, 24]

Statistical analysis

All data are shown as the mean with standard deviation (SD) and all statistical analyses were performed using SPSS for Windows, release 20.0 (SPSS Inc., Chicago, IL, USA) with a Student's *t*-test. A *P* value of less than 0.05 was set as the threshold for statistical significance.

Results and discussion

Synthesis of AD-*g*-HPG and CD-*g*-Dex

Under the catalysis of DMAP, an acetylation reaction occurred between AD and HPG. The results in Table 1 show that the substitute degree of AD increased with an increase in the free ratio of AD to HPG. AD-*g*-HPG did not dissolve in an aqueou solution when the sbustritute degee of AD was up to 19.8%, caused by the hydrophobicity of AD. The structure of AD-*g*-HPG was analyzed using ^{1}H-NMR spectroscopy. As shown in Figure 1, the peaks at 3.4-4.0 ppm was attributed to the

methylene and methine of HPG, and the peak at 4.7 ppm was assigned to hydroxyl group for HPG. Additionally, compared with homopolymer HPG, the peaks at 1.7-2.2 ppm were assigned to the methylene of AD, signifying successful synthesis of AD-*g*-HPG.

Dex was activated to aldehyde Dex after oxidation with $NaIO_4$. Aldehyde Dex conjugated with amino group of mono-6-deoxy-6-ethylenediamino-*β*-CD to prepare CD-*g*-Dex. As shown in Figure 2, the characteric peaks at 3.0-4.0 ppm were assigned to hydrogen proton of suger residues in Dex, and the peak at 4.95 ppm assigned to hydrogen proton of pyranose ring on the C1. Compared with Dex, the peak at 5.07 ppm was representative for hydrogen proton of *β*-CD on C1, indicating the formation of CD-*g*-Dex. In addition, the grafting of *β*-CD onto Dex was also confirmed by FT-IR spectroscopy (Figure 3). As shown in Figure 3, in the spectrum of Dex, an intense band at 3200-3500 cm^{-1} was assigned to the -OH stretching band. A peak between 2900 and 3000 cm^{-1} represented the C-H stretching band, and the peaks at around 1650 and 1018 cm^{-1} were attributed to the stretching of C-O-C. Comparing with Dex, the intensities of the -OH absorption band and the C-H stretching band in the CD-*g*-Dex strengthened. The appearance of stretching of C-O in the range of 1022-1159 cm^{-1} and the peak located at 704 cm^{-1} assigned to -NH indicated the introduction of *β*-CD to Dex.[25]

In situ formation and characterization of hydrogels

Based on the host-guest interaction, supramolecular AD-*g*-HPG/CD-*g*-Dex hydrogel was synthesized using *β*-CD as a host and AD as a guest. The hydrogels with different

compositions were obtained by modifying the mass ratio of AD-*g*-HPG to CD-*g*-Dex. As shown in Table 1, the substitution degree of AD for AD-*g*-HPG10, AD-*g*-HPG5 and AD-*g*-HPG2.5 was 6.7%, 10.5% and 19.8%, respectively. According to the gelation of hydrogel with different compositions (Table 2), we found that the hydrogel could be formed at the current concentrates when the substitution degree of AD in AD-*g*-HPG was 10.5%, whereas no hydrogel was formed when the substitution degree of AD in AD-*g*-HPG was 6.7% and 19.8% and the polymer concentration was less than 20%, indicating the substitution degree of AD plays an important role in the formation of hydrogel. In fact, the interaction between AD and *β*-CD is too weak to trig the formation of hydrogel when AD-*g*-HPG contained less hydrophobic AD. Also, AD-*g*-HPG with more hydrophobic AD self-assembled to nanoaggregates in aqueous solution, which could not promote the formation of hydrogel. Therefore, the gelation of hydrogel was dependent on not only the concentration of polymers but also the substitute degree of AD.

To make a further evaluation of their structure, FT-IR spectrum of AD-*g*-HPG/CD-*g*-Dex hydrogel was carried out (Figure 4). Compared with AD-*g*-HPG, the typical peak at 3200-3500 cm^{-1} assigned to the -OH stretching band, 2900-3000 cm^{-1} attributed to the C-H stretching band and 1022-1159 cm^{-1} due to C-O stretching band in CD-*g*-Dex were found in the hydrogel. Meanwhile, a 1720 cm^{-1} band for C=O stretching vibration in AD-*g*-HPG appeared, suggesting the successful preparation of AD-*g*-HPG/CD-*g*-Dex hydrogel.

Rheology property

As shown in Figure 5, for all of the AD-*g*-HPG/CD-*g*-Dex hydrogels, their G' were greater than G'' indicating the formation of supramolecular hydrogel. The G' was in the range of 600-1600 Pa while the G'' was between 50 and 400 Pa. According to rheology curves of AD-*g*-HPG5/CD-*g*-Dex10, AD-*g*-HPG5/CD-*g*-Dex15 and AD-*g*-HPG5/CD-*g*-Dex20, we found that the G' increased with enhancing β-CD amount in the hydrogel. Similarly, based on the rheology curves of AD-*g*-HPG10/CD-*g*-Dex20, AD-*g*-HPG5/CD-*g*-Dex20 and AD-*g*-HPG2.5/CD-*g*-Dex20, the G' increased as the amount of AD in the hydrogel enhanced (Table 2). Therefore, it can be concluded that the host-guest interaction not only provides a simple strategy to gelation but also obtains excellent mechanical strength of such formed hydrogels.

Morphology of hydrogels

The morphologies of AD-*g*-HPG/CD-*g*-Dex hydrogels in micro scales were observed by SEM. As shown in Figure 6, the SEM images of hydrogel exhibited a highly porous sponge like structure, and the average pore size was between 2 and 10 μm. In fact, the "pores" may provide pockets for water molecules to be included by surface tension for achieving optimal solvation and swelling necessary for gelation.[26] Porous structures of AD-*g*-HPG/CD-*g*-Dex hydrogel not only provide a moist environment for cell proliferation but also facilitate drug loading and release.

Swelling assay

Hydrophilicity is an important property for the hydrogels. Excellent water uptake ability of a material facilitates both cell attachment and penetration during in vitro cell

culturing. To determine their hydrophilicity, we explored the swelling of AD-*g*-HPG/CD-*g*-Dex hydrogels. Figure 7 showed swelling kinetic curves of the hydrogel in pH 7.4 PBS at 37 °C. The swelling ratio of the hydrogels was up to 185% after 2 min of incubation. For the hydrogels with the same the material content, the swelling ratio increased from 130% to 167% when the AD content decreased from 19.8 % to 6.7%, indicating that AD content plays an important role in the water uptake of AD-*g*-HPG/CD-*g*-Dex hydrogels. For the hydrogels contained AD-*g*-HPG5, the equilibrium swelling ratio was only 163% when the concentration increased to 20 mg/mL. The hydrogels prepared at a high concentration had a tighter structure and a higher water-holding capacity. The previous research showed that the more content of materials, the smaller porous structure, and the swelling process in aqueous solution may be lower,[27] which is in accordance with our result.

Degradability of AD-*g*-HPG/CD-*g*-Dex hydrogel

For further in vivo application, the hydrogel degradation was carried out in pH 7.4 PBS at 37 °C. The weight loss of hydrogels was shown in Figure 8, the degradation of AD-*g*-HPG/CD-*g*-Dex hydrogel gradually increased over the time. The 5-10 wt % hydrogel was degraded within 1 day, while the 20-50 wt % hydrogel samples were lost within 7 days. The rapid weight loss of the samples in the first time is probably due to diffusion of un-crosslinked polymeric chains from inside the hydrogel into PBS. One week later, the degradation speed declined. Comparing the weight loss of AD-*g*-HPG10/CD-*g*-Dex20, AD-*g*-HPG5/CD-*g*-Dex20 and AD-*g*-HPG2.5/CD-*g*-Dex20, the degradation degree increased with the increase of

AD amount in hydrogel, implying that the cross-linking density between *β*-CD and AD plays an important role in their degradation. Appropriate degradation time makes hydrogels promising applications for tissue engineering and drug delivery system.

Thermo gravimetric analysis

The TG and DTG curves for AD-*g*-HPG/CD-*g*-Dex are shown in Figure 9. The temperature increased by 10 °C/min from room temperature to 1000 °C. As seen from TG curves, the thermal decomposition of the hydrogels took place in 4 stages. 7% to 9% weight loss of the hydrogel below 100 °C was attributable to free water and water linked through hydrogen bonds. There was 3-4% weight loss observed within the approximate temperature range 200-250 °C, which was caused by oxidized Dex.[28] 10-35% weight loss of the hydrogels occurred in the 250-350 °C region, which was assigned to thermal decomposition of HPG and CD.[29-31] The final decomposition from 350 to 430 °C was related to the degradation of C-C on hydrogels' main chain and AD.

In vitro insulin release study

Figure 10 indicated the insulin release from insulin-loaded hydrogel in pH 7.4 PBS at 37 °C. The percentage of cumulative release was the cumulative amount of insulin released at certain times dividing the total amount of insulin encapsulated in the hydrogel. The release showed two phase model, that was initially rapid release and subsequently stained release. The initially rapid release was caused by some of the insulin adsorbed onto the hydrogel surface. Lately, insulin was released slowly until hydrogels completely degraded or dissolved in release medium. Insulin released from

AD-*g*-HPG10/CD-*g*-Dex20, AD-*g*-HPG5/CD-*g*-Dex10, AD-*g*-HPG5/CD-*g*-Dex15, AD-*g*-HPG5/CD-*g*-Dex20 and AD-*g*-HPG2.5/CD-*g*-Dex20 was about 72%, 78%, 74%, 68% and 65% within the initial 10 h, respectively. As it can be seen, the rate of insulin release from AD-*g*-HPG2.5/CD-*g*-Dex20 reached the minimum due to the fact that a tight network retarded insulin release effectively. This is because this hydrogel contained the most AD comparing with other hydrogels, indicating that more AD formed closer three-dimensional networks, which could delay protein macromolecules releasing, which is in accordance with the results reported.[32]

Furthermore, to determine the in vitro release mechanism of insulin from AD-*g*-HPG/CD-*g*-Dex hydrogel, the following Ritger-Peppas equation was used to fit the data of cumulative release.[33]

$$\frac{M_t}{M_\infty} = Kt^n$$

where M_t/M_∞ is the drug releasing percentage at time t and equilibrium respectively. K is a kinetic rate constant characteristic of the polymer-drug interaction and n is the diffusional exponent to classify the release mechanism. When a plot is drawn between ln (M_t/M_∞) and ln t, the slope of the plot gives value of K and intercept gives value of n. While $n \leqslant 0.43$, the release mechanism is mainly to be Fickian diffusion; if $0.43 < n < 0.85$, non-Fickian transport occurs. Particularly, for $n \geqslant 0.85$, matrix erosion and diffusion is possible.[34]

According to the drug release kinetic data (Table 3), it is noteworthy that, the n values of all AD-*g*-HPG/CD-*g*-Dex hydrogels were between 0.43 and 0.85, demonstrating that release mechanism of insulin from these hydrogels was proved to

mainly obey non-Fickian diffusion, where polymer relaxation and drug diffusion played important roles in drug release. The release mechanism is in accordance with the result reported by Anirudhan et al.[35]

Stability of the release insulin

Circular dichroism spectroscopy is used to evaluate the conformational changes of insulin.[36] The far UV circular dichroism band at 208 nm primarily arises from α-helix structure, while that at 223 nm is for β-structure. The ratio between both bands can be used to generate a qualitative measure of the overall conformational structure of insulin. In the present work, as shown in Figure 11, the ratio for standard insulin and released insulin were 1.23 and 1.24, respectively, indicating that there was no significant conformational change observed for the released insulin from the hydrogel at pH 7.4 comparing with the standard insulin. Moreover, this indicates that both the distinctive tertiary structure and biological activity of insulin were kept to optimal after encapsulated and released from the hydrogel.

Cytotoxicity

The cytotoxicity of AD-*g*-HPG/CD-*g*-Dex hydrogel was investigated in NIH 3T3 cells using MTT method. The cells without the hydrogel treatment were considered as control and their viability was set 100%. The NIH 3T3 cells were incubated with the hydrogel leaching solution with different concentrations for 48 h. As shown in Figure 12, the cell viability of NIH 3T3 after the treatment of hydrogel showed more than 80% after the incubation of 48 h, indicating that the hydrogel promoted the cell proliferation. Importantly, AD-*g*-HPG5/CD-*g*-Dex20 exhibited significantly higher

cell viability compared with other samples at the concentration of 0.625 mg/mL. This is because AD-*g*-HPG5/CD-*g*-Dex20 hydrogel contains the more contents of polysaccharide Dex than other samples. Most possibly, polysaccharide Dex is similar to glycosaminoglycan that is an important constituent of ECM and promotes cell proliferation. The results suggest that AD-*g*-HPG/CD-*g*-Dex have a potential application for drug delivery and tissue engineering.

Cell viability assay

Since the above results displayed AD-*g*-HPG/CD-*g*-Dex hydrogels with good biocompatibility, we further evaluated them for cell culture. Mouse fibroblast NIH 3T3 cells were added in a 12-well plate during the formation of the hydrogel and then a LIVE/DEAD assay was carried out. As shown in Figure 13A, a vast majority of the encapsulated cells showed natural fusiform shape and were alive, as indicated by most of the cells showing a green color. This is because live and dead cells could only be stained by dyes of AO (emits green light) and EB (emits red light), respectively. These observations indicate that this supramolecular hydrogel was suitable for cell culture in 3D environments.

Conclusions

In the present work, we have synthesized a new supramolecular hydrogel AD-*g*-HPG/CD-*g*-Dex which had typical porous structure and ideal three-dimensional network via host-guest interaction. The porous structure made the hydrogel excellent protein encapsulation and controlled drug release. Improtantly, the hydrogel mimicking the ECM could promote cell proliferation. Therefore,

AD-*g*-HPG/CD-*g*-Dex hydrogel has promising and useful applications for tissue engineering and drug delivery system.

Acknowledgements

This work was supported by the National Natural Science Foundation of China (Grant 81170773), The National High Technology Research and Development 863 Program of China (Grant 2012AA022602) and Wu Jieping Medical Foundation (320675012173 to Zhongming Wu).

References

1 Z. B. Li, H. Yin, Z. X. Zhang, K. L. Liu and J. Li, *Biomacromolecules*, 2012, **13**, 3162-3172.

2 D. W. Wu, T. Wang, B. Lu, X. D. Xu, S. X. Cheng, X. Z. Zhang and R. Z. Zhuo, *Langmuir*, 2008, **24**, 10306-10312.

3 D. Ma, Kai. Tu and L. M. Zhang, *Biomacromolecules*, 2010, **11**, 2204-2212.

4 Y. G. Jia and X. X. Zhu, *Chem. Mater.*, 2015, **27**, 387-393.

5 Z. X. Zhang, K. L. Liu and J. Li, *Angew. Chem. Int. Ed.*, 2013, **52**, 6180-6184.

6 E. A. Appel, F. Biedermann, U. Rauwald, S. T. Jones, J. M. Zayed and O. A. Scherman, *J. Am. Chem. Soc.*, 2010, **132**, 14251-14260.

7 Q. Wei, T. Becherer, R. C. Mutihac, P. L. M. Noeske, F. Paulus, R. Haag and I. Grunwald, *Biomacromolecules*, 2014, **15**, 3061-3071.

8 T. Loftsson and M. E. Brewster, *J. Pharm. Pharmacol.*, 2011, **63**, 1119-1135.

9 G. C. Yu, K. C. Jie and F. H. Huang, *Chemi. Rev.*, 2015, **115**, 7240-7303.

10 C. Siegers, M. Biesalski and R. Haag, *Chem. Eur. J.*, 2004, **10**, 2831-2838.

11 M. Weinhart, T. Becherer, N. Schurbusch, K. Schwibbert, H. J. Kunte and R. Haag, *Adv. Eng. Mater.*, 2011, **13**, B501-B510.

12 M. Lange, S. Braune, K. Luetzow, K. Richau, N. Scharnagl, M. Weinhart, A. T. Neffe, F. Jung, R.Haag and A. Lendlein, *Macromol. Rapid. Commun.*, 2012, **33**, 1487-1492.

13 J. Khandare, A. Mohr, M. Calderón, P. Welker, K. Licha and R. Haag, *Biomaterials*, 2010, **31**, 4268-4277.

14 A. Sunder, R. Hanselmann, H. Frey and R. Mülhaupt, *Macromolecules*, 1999, **32**, 4240-4246.

15 B. May, S. Kean, C. Easton and S. Lincoln, *J. Chem. Soc. Perkin Trans. 1*, 1997, **21**, 3157-3160.

16 Y. Y. Liu, X. D. Fan and L. Gao, *Macromol. Biosci.*, 2003, **3**, 715-719.

17 X. G. Zhang, Z. M. Wu, X. J. Gao, S. J. Shu, H. J. Zhang, Z. Wang and C. X. Li, *Carbohyd. Polym.*, 2009, **77**, 394-401.

18 B. Jeong, Y. H. Bae and S. W. Kim, *Macromolecules*, 1999, **32**, 7064-7069.

19 D. Y. Teng, Z. M. Wu, X. G. Zhang, Y. X. Wang, C. Zheng, Z. Wang and C. X. Li, *J. Polym. Res.*, 2010, **51**, 639-646.

20 S. Hashmi, A. GhavamiNejad, F. O. Obiweluozor, M. Vatankhah-Varnoosfaderani and F. J. Stadler, *Macromolecules*, 2012, **45**, 9804-9815.

21 M. M. Bradford, *Anal. Biochem.*, 1976, **72**, 248-254.

22 S. M. Kelly, T. J. Jess and N. C. Price, *BBA- Proteins Proteom.*, 2005, **1751**, 119-139.

23 R. Loganathan, S. Ramakrishnan, E. Suresh, A. Riyasdeen, M. A. Akbarsha and M. Palaniandavar, *Inorg. Chem.*, 2012, **51**, 5512-5532.

24 R. Sethu, R. Venugopal, P. Mallayan, S. P. Vaiyapuri, S. S. Bangalore, K. Hanumanthappa, and A. A. Mohammad, *Inorg. Chem.*, 2009, **48**, 1309-1322.

25 X. J. Zhang, X. G. Zhang, Z. M. Wu, X. J. Gao, C. Cheng, Z. Wang and C. X. Li, *Acta Biomater.*, 2011, **7**, 585-592.

26 S. Bhattacharya and S. G. Acharya, *Chem. Mat.*, 1999, **11**, 3504-3511.

27 L. E. Nita, M. T. Nistor, A. P. Chiriac and I. Neamtu, *Ind. Eng. Chem. Res.*, 2012, **51**, 7769-7776.

28 J. Maia, R. A. Carvalho, J. F. J. Coelho, P. N. Simões and M. H. Gil, *Polymer*, 2011, **52**, 258-265.

29 A. Azzouz, N. Platon, S. Nousir, K. Ghomari, D. Nistor, T. C. Shiao and R. Roy, *Sep. Purif. Technol.*, 2013, **108**, 181-188.

30 S. Krishnamoorthi, D. Mal and R. P. Singh, *Carbohyd. Polym.*, 2007, **69**, 371-377.

31 T. R. Thatiparti, A. J. Shoffstall and H. A. von Recum, *Biomaterials*, 2010, **31**, 2335-2347.

32 Z. M. Wu, X. G. Zhang, C. Zheng, C. X. Li, S. M. Zhang, R. N. Dong and D. M. Yu, *Eur. J. Pharm. Sci.*, 2009, **37**, 198-206.

33 A. M. Zalfen, D. Nizet, C. Jerome, R. Jerome, F. Frankenne, J. M. Foidart, V. Maquet, F. Lecomte, P. Hubert and B. Evrard, *Acta Biomater.*, 2008, **4**, 1788-1796.

34 J. Siepmann and N. A. Peppas. *Adv. Drug Deliv. Rev.*, 2001, **48**, 139-157.

35 T. S. Anirudhan, P. L. Divya and J. Nima, *Mat. Sci. Eng. C*, 2015, **55**, 471-481.

36 X. J. Jin, X. G. Zhang, Z. M. Wu, D. Y. Teng, X. J. Zhang, Y. X. Wang, Z. Wang and C. X. Li, *Biomacromolecules*, 2009, **10**, 1337-1345.

Table 1. The synthesis of AD-*g*-HPG with different compositions

Sample	-OH: Ada (mol/mol)	DS (%) [a]	Yield (%)
AD-*g*-HPG10	10:1	6.7	68
AD-*g*-HPG5	5:1	10.5	57
AD-*g*-HPG2.5	5:2	19.8	50

[a] DS referred to degree of substitution and was calculated through elemental analysis.

Table 2. Gelation of hydrogel with different compositions

AD-*g*-HPG	AD-*g*-HPG/CD-*g*-Dex(%)		
	10%	15%	20%
AD-*g*-HPG10	---	---	AD-*g*-HPG10/CD-*g*-Dex20
AD-*g*-HPG5	AD-*g*-HPG5/CD-*g*-Dex10	AD-*g*-HPG5/CD-*g*-Dex15	AD-*g*-HPG5/CD-*g*-Dex20
AD-*g*-HPG2.5	---	---	AD-*g*-HPG2.5/CD-*g*-Dex20

--- cannot get hydrogel

Table 3. Drug release kinetic data of AD-*g*-HPG/CD-*g*-Dex hydrogel via fitting drug release experimental data to Ritger-Peppas equation

Sample	Ridger-Peppas model			Transport mechanism
	K	*n*	R^2	
AD-*g*-HPG10/CD-*g*-Dex20	2.70	0.51	0.98	non-Fickian diffusion
AD-*g*-HPG5/CD-*g*-Dex10	4.69	0.44	0.99	non-Fickian diffusion
AD-*g*-HPG5/CD-*g*-Dex15	3.27	0.48	0.98	non-Fickian diffusion
AD-*g*-HPG5/CD-*g*-Dex20	1.98	0.55	0.98	non-Fickian diffusion
AD-*g*-HPG2.5/CD-*g*-Dex20	1.82	0.56	0.98	non-Fickian diffusion

Figure captions

Figure 1. ^{1}H NMR spectra of HPG and AD-*g*-HPG.

Figure 2. ^{1}H NMR spectra of Dex and CD-*g*-Dex.

Figure 3. FT-IR spectra of Dex and CD-*g*-Dex.

Figure 4. FT-IR spectra of AD-*g*-HPG, CD-*g*-Dex and AD-*g*-HPG/CD-*g*-Dex.

Figure 5. Dynamic rheological behaviors of AD-*g*-HPG/CD-*g*-Dex.

Figure 6. SEM images of AD-*g*-HPG/CD-*g*-Dex: (A) AD-*g*-HPG10/CD-*g*-Dex20;
(B) AD-*g*-HPG5/CD-*g*-Dex10; (C) AD-*g*-HPG5/CD-*g*-Dex15;
(D) AD-*g*-HPG5/CD-*g*-Dex20 and (E) AD-*g*-HPG2.5/CD-*g*-Dex20.

Figure 7. Swelling percentages of AD-*g*-HPG/CD-*g*-Dex in pH 7.4 PBS.

Figure 8. Weight loss of AD-*g*-HPG/CD-*g*-Dex hydrogel samples in PBS versus immersion time.

Figure 9. TG (A) and DTG (B) curves of AD-*g*-HPG/CD-*g*-Dex.

Figure 10. In vitro percentage cumulative release of insulin from AD-*g*-HPG/CD-*g*-Dex in pH 7.4 PBS.

Figure 11. Circular dichroism spectra of released insulin and standard insulin.

Figure 12. Cell viability after incubation with different concentrations of AD-*g*-HPG/CD-*g*-Dex determined by MTT assay for 48 h. Data were presented as mean ± SD (n = 5). There was significant difference set as *$P<0.05$; **$P<0.01$; ***$P<0.001$.

Figure 13. The micrographs of AO/EB-stained NIH3T3 cells after encapsulated in AD-*g*-HPG5/CD-*g*-Dex20 hydrogel at a concentration of 5×10^{4} cells/mL for 48 h. (A)

no fluorescence excitation and (B) with fluorescence excitation.

Figure 1

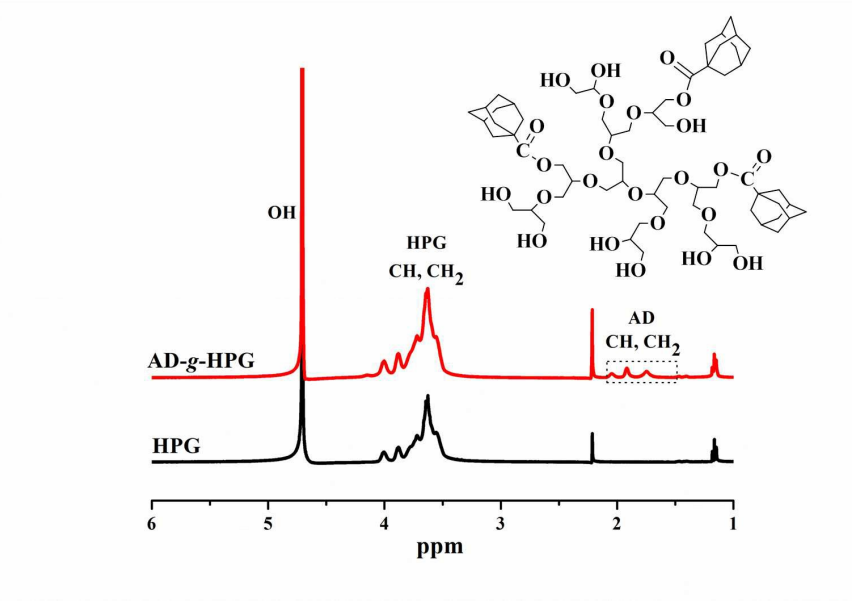

643 Figure 2

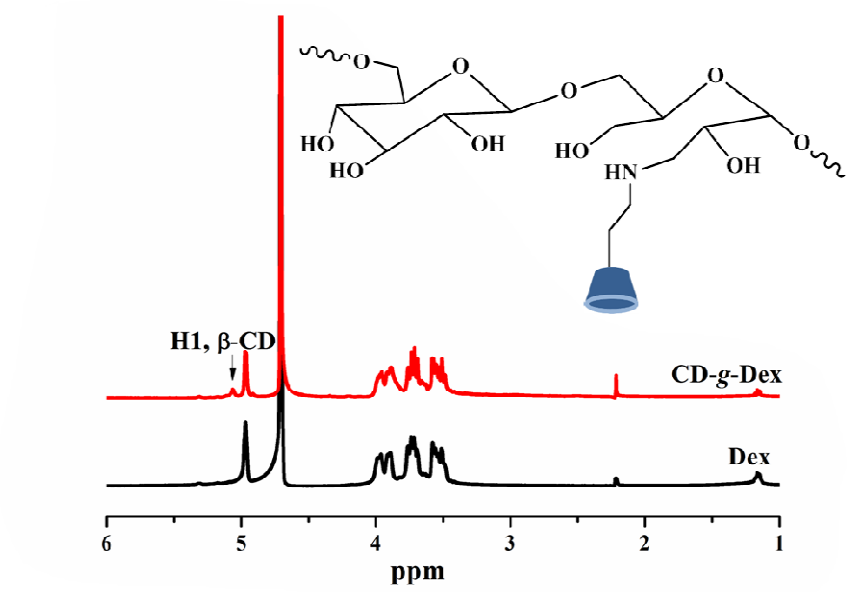

644
645
646
647
648
649
650
651
652
653
654
655
656
657
658
659
660
661
662
663
664
665
666
667
668
669
670
671

672

673 Figure 3

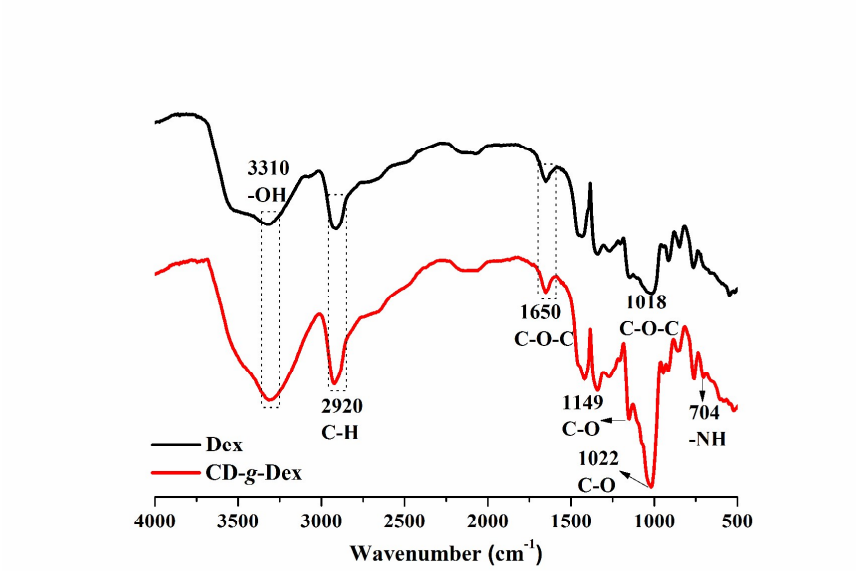

674

675

676

677

678

679

680

681

682

683

684

685

686

687

688

689

690

691

692

693 Figure 4

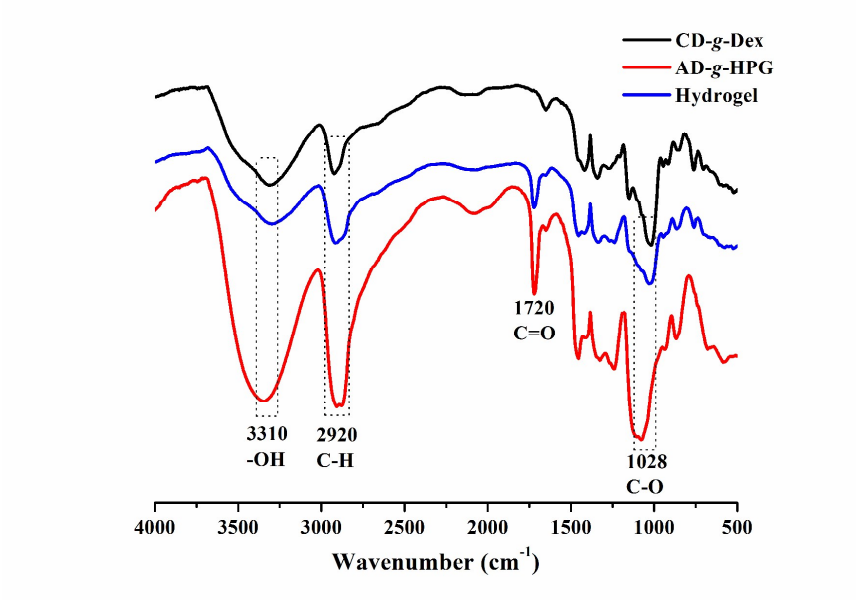

694

695

696

697

698

699

700

701

702

703

704

705

706

707

Figure 5

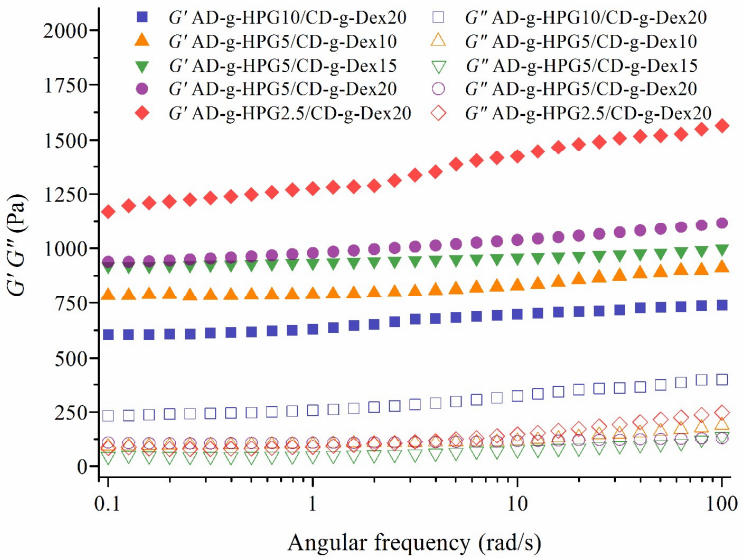

723 Figure 6

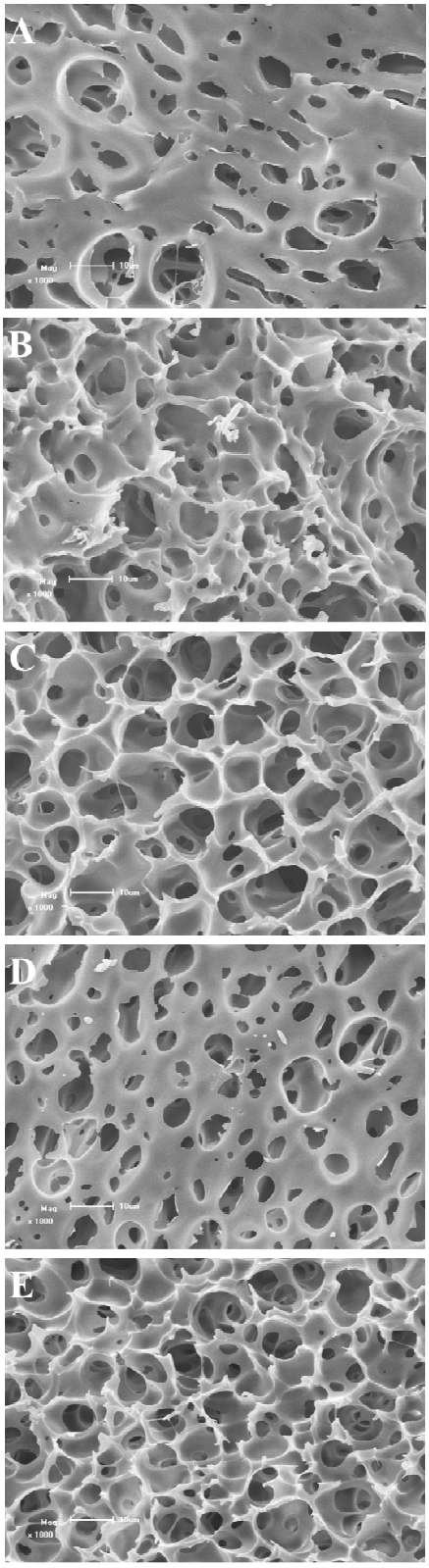

724
725
726
727
728
729

Figure 7

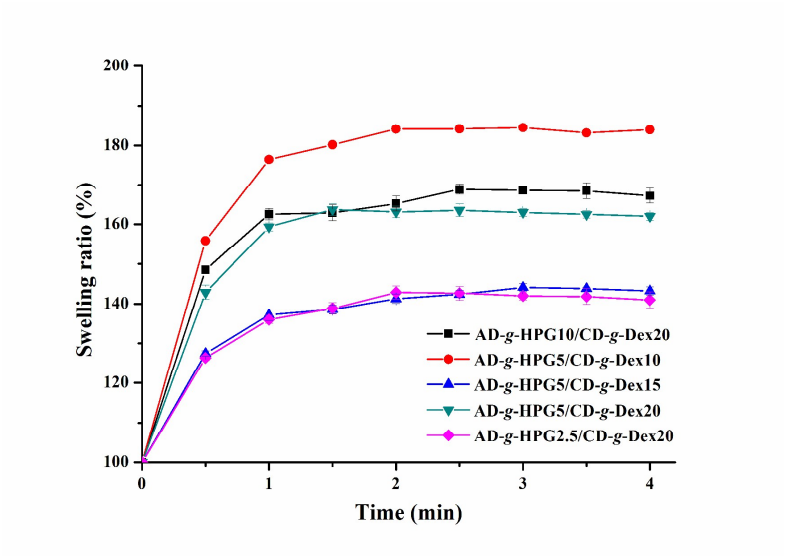

Figure 8

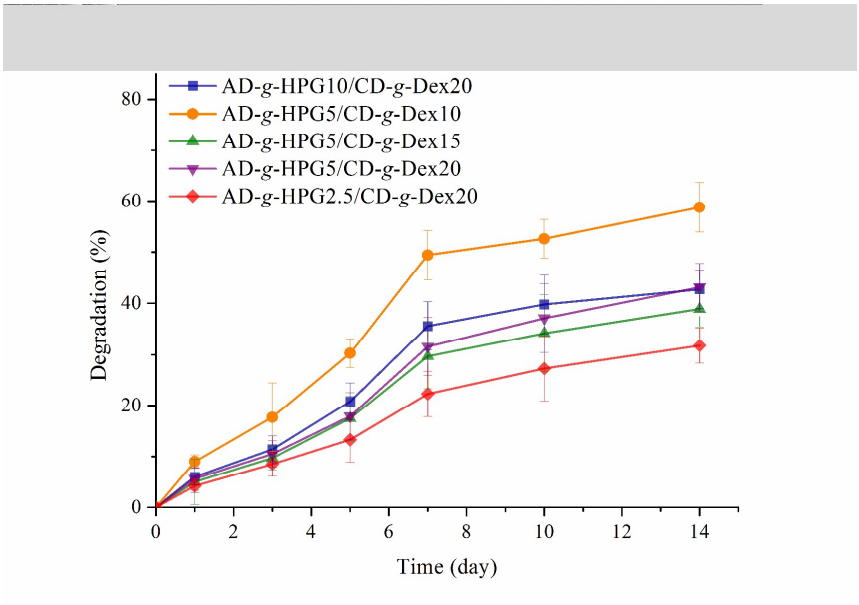

789 Figure 9

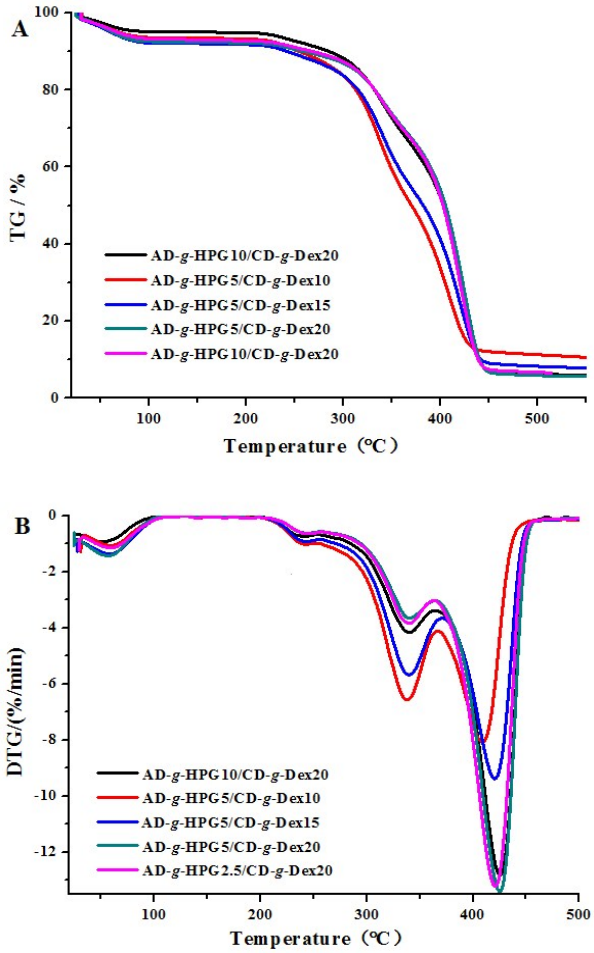

790
791
792
793
794
795
796
797
798
799
800
801
802
803
804
805
806
807
808
809

Figure 10

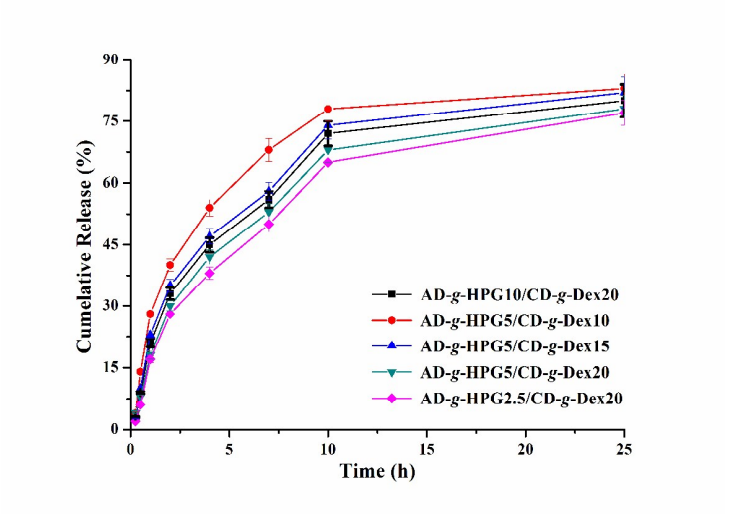

832 Figure 11

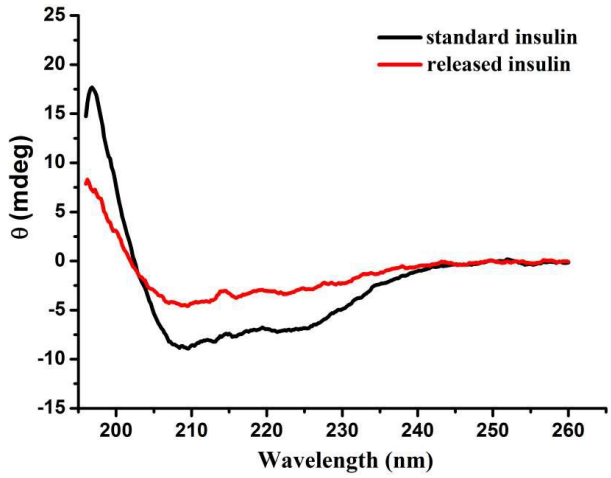

833

834

835

836

837

838

839

840

841

842

843

844

845

846

847

848

Figure 12

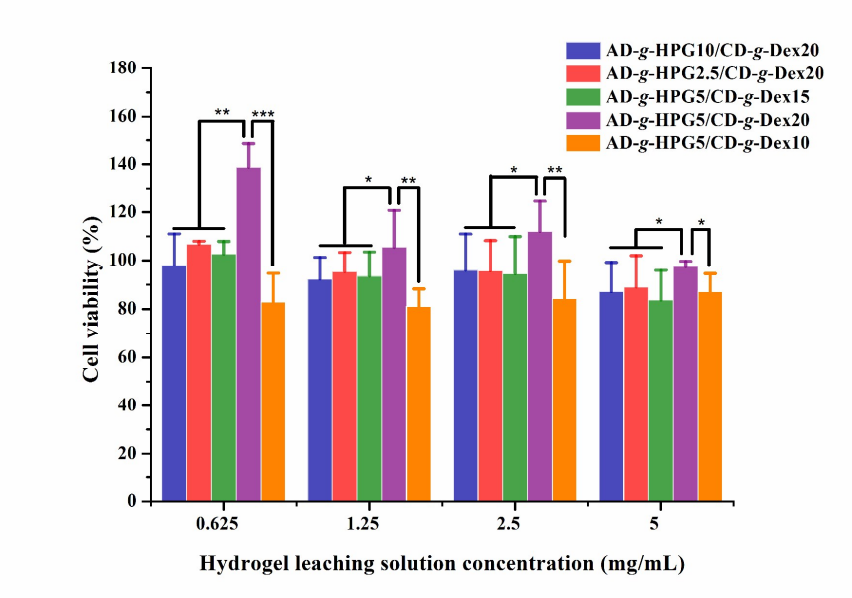

877 Figure 13

878

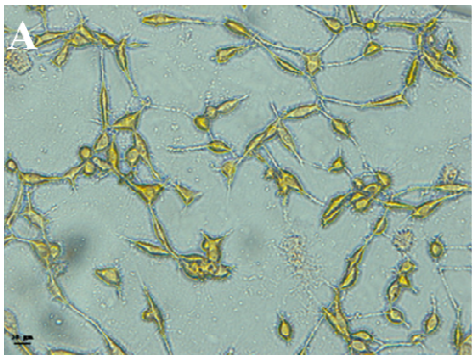

879